ドキソルビシン耐性濾胞樹状細胞肉腫のヒト由来同所移植マウスモデルにおけるテモゾロミドの有効性の検討

Tissue and Cell 58 (2019) 17–23

Contents lists available at ScienceDirect

Tissue and Cell

journal homepage: www.elsevier.com/locate/tice

Temozolomide targets and arrests a doxorubicin-resistant follicular dendritic-cell sarcoma patient-derived orthotopic xenograft mouse model

Hiromichi Oshiro[a,b,c], Yasunori Tome[c,*], Tasuku Kiyuna[a,b,c], Kentaro Miyake[a,b], Kei Kawaguchi[a,b], Takashi Higuchi[a,b], Masuyo Miyake[a,b], Zhiying Zang[a,b], Sahar Razmjooei[a,b], Maryam Barangi[a,b], Sintawat Wangsiricharoen[a,b], Scott D. Nelson[d], Yunfeng Li[d], Michael Bouvet[b], Shree Ram Singh[e,*], Fuminori Kanaya[c], Robert M. Hoffman[a,b,*]

[a] AntiCancer Inc., San Diego, CA, USA
[b] Department of Surgery, University of California, San Diego, CA, USA
[c] Department of Orthopedic Surgery, Graduate School of Medicine, University of the Ryukyus, Okinawa, Japan
[d] Department of Pathology, University of California, Los Angeles, CA, USA
[e] Basic Research Laboratory, National Cancer Institute, Frederick, MD, USA

ARTICLE INFO

Keywords:
Follicular dendritic cell sarcoma
Soft-tissue
Patient-derived orthotopic xenograft
PDOX
Temozolomide
Doxorubicin

ABSTRACT

Follicular dendritic cell sarcoma (FDCS) is a very rare and highly recalcitrant disease. A patient's doxorubicin-resistant FDCS was previously established orthotopically on the right high thigh into the biceps femoris of mice to establish a patient-derived orthotopic xenograft (PDOX) model. The aim of the present manuscript was to identify an effective drug for this recalcitrant tumor. Here, we evaluated the efficacy of temozolomide (TMZ), trabectedin (TRAB) and pazopanib (PAZ) on the FDCS PDOX model. PDOX mouse models were randomized into five groups of eight to nine mice, respectively. Group 1, untreated control with PBS, i.p.; Group 2, treated with doxorubicin (DOX), 2.4 mg/kg, i.p., weekly for 3 weeks; Group 3, treated with PAZ, 50 mg/kg, oral gavage, daily for 3 weeks; Group 4, treated with TMZ, 25 mg/kg, oral gavage, daily for 3 weeks; Group 5, treated with TRAB, 0.15 mg/kg, i.v., weekly for 3 weeks. Body weight and tumor volume were assessed 2 times per week. TMZ arrested the FDCS PDOX model compared to the control group ($p < 0.05$). PAZ and TRAB did not have significant efficacy compared to the control group ($p = 0.99$, $p = 0.69$ respectively). The PDOX tumor was resistant to DOX ($p = 0.99$). as was the patient. The present study demonstrates that TMZ is effective for a PDOX model of FDCS established from a patient who failed DOX treatment, further demonstrating the power of PDOX to identify effective therapy including for tumors that failed first line therapy.

1. Introduction

Follicular dendritic cell sarcoma (FDCS) is a very rare and recalcitrant cancer with, which was first reported in 1986 by Monda et al. (1986). FDCS is recognized as a diagnostically-challenging neoplasm and has greater malignant potential than initially thought. FDCS often develops in cervical, mediastinal or axillary lymph nodes. In nearly one-third of cases, FDCS can also occur in extra-nodal sites (Chen and Gopal, 2017; Duan et al., 2010; Biddle et al., 2002; Soriano et al., 2007; Davila et al., 2017; Hassan et al., 2018; Walters et al., 2018). Several markers were suggested as diagnostic marker for FDCS such as CD137 (Anderson et al., 2012), CD23 (Chen and Gopal, 2017), estrogen receptor (ER)-α (Sapino et al., 2003), clusterin (Grogg et al., 2004), chemokine (C-X-C motif) ligand 13 (CXCL13), CD21, CD35, follicular dendritic cell secreted protein (FDCSP), serglycin (SRGN) (Lorenzi et al., 2017), mouse double minute 2 homolog (MDM2) and somatostatin receptor 2A [SSTR2A]) (Agaimy et al., 2016). FDCS has been linked with extensive chromosomal instability, cell cycle progression defect, with mutations of v-Raf murine sarcoma viral oncogene homolog B (BRAF), activation of nuclear factor kappa beta (NF-kB), activation of mitogen-activated protein kinase (MAPK), overexpression of epidermal growth factor receptor (EGFR), neurofibromatosis type 2 (NF2) mutation, and immune evasion (Agaimy et al., 2016; Griffin et al., 2016; Sun et al., 2003; Go et al., 2014; Andersen et al., 2017; Karrs et al., 2018). The most frequent reported systemic therapy is C/EBP homologous protein (CHOP) chemotherapy, which contains cyclophosphamide, doxorubicin (DOX), vincristine, and prednisolone with generally poor outcome (Conry, 2014a; Dan et al., 2014; Khalid

* Corresponding authors at: AntiCancer Inc., San Diego, CA, USA.
E-mail addresses: yash_toume@hotmail.com (Y. Tome), singhshr@mail.nih.gov (S.R. Singh), all@anticancer.com (R.M. Hoffman).

https://doi.org/10.1016/j.tice.2019.04.002
Received 25 March 2019; Accepted 1 April 2019
Available online 03 April 2019
0040-8166/ Published by Elsevier Ltd.

and Folman, 2005; Shinagare et al., 2011). Therefore, novel approaches for FDCS are needed.

Temozolomide (TMZ) is an imidazotetrazine alkylating agent. TMZ is a small molecule (molecular weight of 194 Daltons). TMZ is easily absorbed in the digestive tract after oral administration, and its bioavailability is almost 100%. TMZ is lipophilic and can easily cross the blood-brain barrier (Simonetti et al., 2014). TMZ is approved for melanoma and refractory anaplastic astrocytoma (Keir et al., 2013; Setty et al., 2018; Kinoshita et al., 2018; Bupathi et al., 2017). TMZ is also a promising target in small cell lung cancer (SCLC) (Lok et al., 2017); melanoma (Kawaguchi et al., 2017a); undifferentiated spindle-cell sarcoma (Igarashi et al., 2018a); myxofibrosarcoma (Kiyuna et al., 2018); Ewing's sarcoma (Palmerini et al., 2018) alveolar rhabdomyosarcoma (Kinoshita et al., 2018); and rhabdomysarcoma (Igarashi et al., 2017a).

Trabectedin (TRAB), an alkylating agent, was initially isolated from the marine ascidian *Ecteinascidia turbinate* (Cuevas and Francesch, 2009). TRAB has been tested on advanced liposarcoma and leiomyosarcoma patient (Demetri et al., 2016; Kawai et al., 2017) and has been marketed for liposarcoma and leiomyosarcoma. TRAB binds to the minor groove of DNA and affects DNA repair pathways, which result in G2-M cell cycle arrest and apoptosis. TRAB showed high efficacy against several soft tissue sarcomas (Le Cesne et al., 2015).

Pazopanib (PAZ) is a small molecule multi-tyrosine kinase inhibitor, blocking various signaling pathways and was tested in a Phase III clinical trial for soft tissue sarcoma (Schoffski, 2012; van der Graaf et al., 2012).

Toward the goal of individualized precision oncology, we have developed the patient-derived orthotopic xenograft (PDOX) nude mouse model for all major cancers (Wang et al., 1992; Yamamoto et al., 2016; Fu et al., 1992; Hiroshima et al., 2014a,b; Fu and Hoffman, 1993; Hiroshima et al., 2015a,b,c; Murakami et al., 2016; 2017; Metildi et al., 2014; Furukawa et al., 1993; Kawaguchi et al., 2017b; Kiyuna et al., 2016; Kawaguchi et al., 2019; Miyake et al., 2017; Igarashi et al., 2018b).

We previously reported that a FDCS PDOX model was resistant to DOX and dactolisib (Kiyuna et al., 2016). However, the FDCS PDOX model was regressed by tumor-targeting *Salmonella typhimurium* A1-R (Kiyuna et al., 2016).

Recently, we have established PDOX models of pleomorphic rhabdomyosarcoma, undifferentiated spindle-cell sarcoma, and lung metastasis of osteosarcoma (Igarashi et al., 2017a,b,c). TMZ, TRAB, and PAZ agents were previously found to be effective on these PDOX models (Igarashi et al., 2017a,b,c).

The aim of the present manuscript was to identify an effective drug for this recalcitrant tumor. In the present study, we evaluated novel therapeutic strategies, using TMZ, DOX, TRAB, and PAZ on the FDCS PDOX model derived from a patient who failed first line DOX chemotherapy.

2. Materials and methods

2.1. Mice

Athymic *nu/nu* nude mice (AntiCancer Inc., San Diego, CA), 4–6 weeks old, were used in this study. Mouse housing, feeding, surgical processes and imaging were conducted as previously described (Kiyuna et al., 2016). The mice were humanely sacrificed as previously described (Kiyuna et al., 2016). All animal studies were conducted with an AntiCancer Institutional Animal Care and Use Committee (IACUC)-protocol specifically approved for this study and in accordance with the principals and procedures outlined in the National Institute of Health Guide for the Care and Use of Animals under Assurance Number A3873-1.

2.2. Patient-derived tumor

In this study, we used a tumor surgical specimen from a female patient diagnosed with recurrent extra-nodal FDCS of the left lower extremity who underwent surgical resection (Kiyuna et al., 2016). She previously received adjuvant radiotherapy to the primary tumor in 2014 and four cycles of chemotherapy with DOX and cyclophosphamide for her recurrent disease (Kiyuna et al., 2016). Details of surgical resection and chemotherapy given to this patient have been previously described (Kiyuna et al., 2016). Written informed consent was obtained from the patient as part of a UCLA Institutional Review Board (IRB #10-001857)-approved protocol (Kiyuna et al., 2016).

2.3. Establishment of a PDOX model of FDCS by surgical orthotopic implantation (SOI)

FDCS sample collection from the patient, performing subcutaneous implantation in nude mice, harvesting tumors from the mice, creating a space at the orthotopic site in the biceps femoris to insert tumor fragments in the mice and to establish the PDOX model and wound-closure procedures have been described in detail in our previous publication (Kiyuna et al., 2016).

2.4. Treatment study design in the FDCS PDOX model

All treatment procedures and data collection were performed as previously reported (Kiyuna et al., 2016). PDOX mouse models were randomized into five groups (Fig. 1A) of eight to nine mice, respectively. Group 1, untreated control, i.p. (n = 9); Group 2, treated with DOX, 2.4 mg/kg, i.p., weekly for 3 weeks (n = 9); Group 3, treated with PAZ, 50 mg/kg, oral gavage, daily for 3 weeks (n = 8); Group 4, treated with TRAB, 0.15 mg/kg, i.v., weekly for 3 weeks (n = 8); Group 5, treated with TMZ, 25 mg/kg, oral gavage, daily for 3 weeks (n = 9). Tumor length, width and mouse body weight were measured with calipers and digital balance, respectively twice a week. Mice were treated for 3 weeks (21 days) in each treatment group, and the final tumor measurement and other analysis was done on day 22. Tumor volume was calculated with the following formula: Tumor volume (mm^3) = length (mm) × width (mm) × width (mm) × 1/2. Data are presented as mean ± SD. The tumor volume ratio is defined at the tumor volume at any given time point relative to the initial tumor volume.

2.5. Histological examination

Fresh tumor samples were fixed in 10% formalin and embedded in paraffin before sectioning and staining. Tissue Sections (5 μm) were deparaffinized in xylene and rehydrated in an ethanol series. Hematoxylin and eosin (H&E) staining was performed according to standard protocol (Murakami et al., 2016).

2.6. Statistical analysis

JMP version 13.0 was used for statistical analyses. Significant differences for continuous variables were determined using the Steel-Dwass test. Line graphs express average values and error bars show ± standard deviation. A probability value of $P < 0.05$ was considered statistically significant.

3. Results

3.1. Efficacy of TMZ, DOX, TRAB, and PAZ on the FDCS PDOX mouse model

The treatment schedule for the PDOX models of FDCS is shown in Fig. 1A. The time-course increase, or inhibition of the tumor volume ratio is shown in Fig. 1B. Figs. 1B and 2B shows the quantitative data

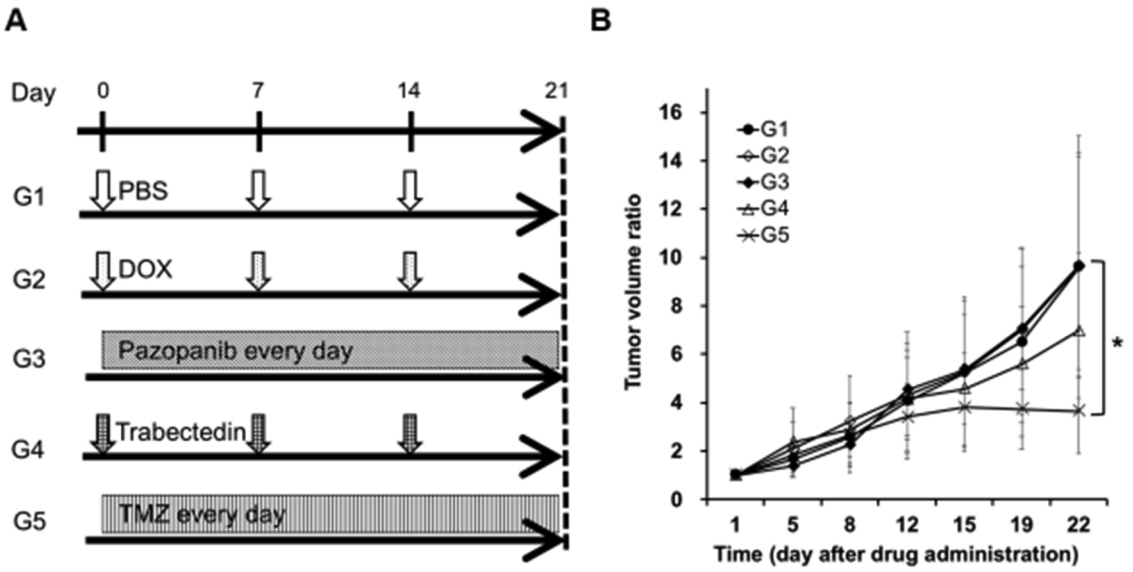

Fig. 1. Treatment schema and drug efficacy on the FDCS PDOX model. (A) A patient FDCS was grown orthotopically in the right biceps femoris of nude mice. Treatment started on day 1st and ended day 22nd. (B) Drug efficacy on the FDCS PDOX model. Line graphs show tumor volume ratio which is the volume of the tumor at the given time points with respect to the initial tumor volume. Line graphs express average and error bars show ± standard deviation. There were statistically significant differences between TMZ and the untreated control, TMZ and DOX, and TMZ and PAZ. Statistical analysis was performed using Steel-Dwass test. *P < 0.05.

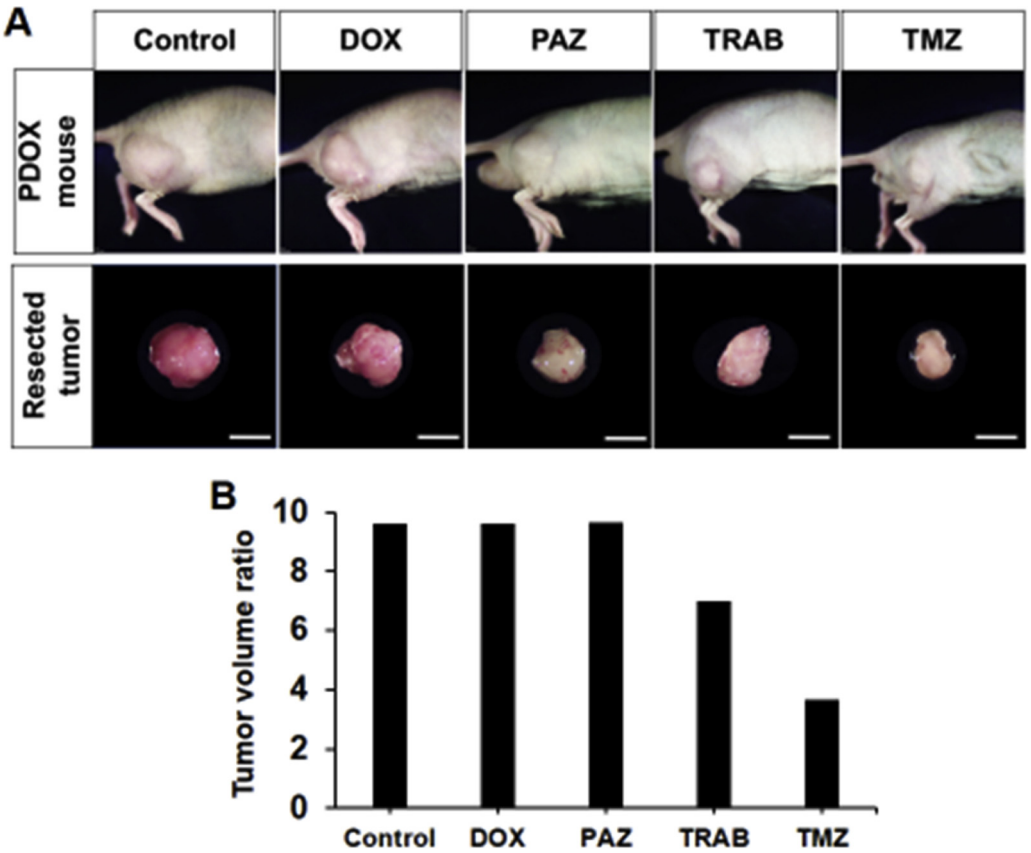

Fig. 2. (A). Photograph of tumors in situ and resected tumors of representative treated and untreated FDCS PDOX models. TMZ arrested the FDCS PDOX model. (B). Line graphs show tumor volume ratio on 22nd day. Scale bars are 10 mm.

from initiation of treatment until end of treatment. Fig. 2A shows the representative tumors in each group. The FDCS PDOX model was resistant to DOX (p = 0.99 at day-22 of treatment, Group 2) and PAZ (p = 0.99 at day-22, Group 3). The FDCS PDOX model was slightly sensitive to TRAB, however, no statistically-significant difference were observed (p = 0.69 at day-22, Group 4). In contrast, the FDCS PDOX model was arrested by TMZ (p < 0.05 at day-22, Group 5). There was a statistically significant difference statistically between TMZ and the untreated control; TMZ and DOX; and TMZ and PAZ.

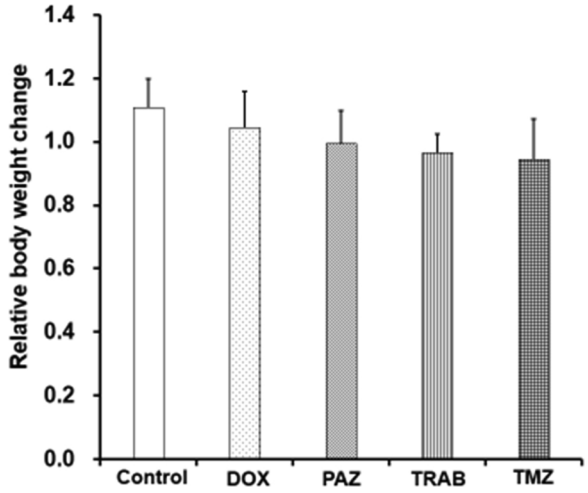

Fig. 3. Effect of treatment on body weight. Bar graphs show the body weight ratio of mice in each group on 22nd day from initial treatment with respect to body weight at start of treatment. Group 1 (untreated control): 1.11 ± 0.09; Group 2 (DOX): 1.04 ± 0.11; Group 3 (PAZ): 0.99 ± 0.11; Group 4 (TRAB): 0.96 ± 0.06; Group 5 (TMZ): 0.95 ± 0.13.

3.2. Body weight

Body weight was used as a general toxicity marker. The body weights at day-21 for all groups were as follows: Group 1 (untreated control with PBS): 27.55 ± 3.15; Group 2 (DOX): 26.70 ± 3.64; Group 3 (PAZ): 27.19 ± 5.35; Group 4 (TRAB): 27.34 ± 3.06; Group 5 (TMZ): 23.68 ± 4.48, respectively. No animal deaths in any group was observed. Moreover, no significant body-weight differences were observed among the groups (Fig. 3).

3.3. Histology

H&E-staining of tumor tissue sections was made from the FDCS PDOX models at the end of the experiment. The untreated-control group showed similar histologic features with the original patient tumor which included relatively uniform spindle-shaped cells present in storiform patterns and admixed chronic inflammatory cells (Fig. 4A). In the PDOX tumor treated with DOX, PAZ or TRAB, cancer cells invading muscle were observed (Fig. 4B, C, D). Necrosis was only detected in PDOX tumors treated with TMZ (Fig. 4E).

4. Discussion

Several studies reported the treatment of FDCS using a combination of gemcitabine and docetaxel (Conry, 2014; Jain et al., 2017), a combination of CHOP, ABVD (DOX, bleomycin, vinblastine, dacarbazine), and ICE (ifosfamide, carboplatin, etoposide) (Biddle et al., 2002; Soriano et al., 2007; Shinagare et al., 2011), ridaforolimus, an mTOR (mammalian target of rapamycin) inhibitor (Mita et al., 2013), anthracycline-based regimens (Gounder et al., 2015), and a poly ADP-ribose polymerase (PARP) inhibitor in combination with carboplatin (Lemech et al., 2016), and bendamustine (Sasaki et al., 2017) and imatinib (Azim et al., 2007).

In the present study, DOX, TMZ, TRAB, and PAZ were tested on the FDCS PDOX model. The FDCS PDOX model was resistant to DOX as well as was the patient. In contrast, with regard to arresting tumor growth and causing tumor necrosis, the present results showed that TMZ was effective on the FDCS PDOX model.

TMZ in combination with talazoparib showed highly promising therapy for SCLC (Bupathi et al., 2017). TMZ regressed a DOX-resistant undifferentiated spindle-cell sarcoma PDOX (Igarashi et al., 2018a). TMZ in combination with bevacizumab showed an effective and tolerated treatment for patients with solitary fibrous tumor (de Lemos et al., 2018). TMZ in combination with irinotecan arrested a DOX and TMZ-resistant myxofibrosarcoma PDOX model and sarcoma PDOX model (Kiyuna et al., 2018). TMZ in combination with vincristine and irinotecan was effective for alveolar rhabdomyosarcoma (Setty et al., 2018).

Our previous studies showed that PAZ and TRAB had significant inhibitory efficacy on the PDOX models of undifferentiated spindle cell sarcoma (Igarashi et al., 2017b) and osteosarcoma lung metastasis (Igarashi et al., 2017c). However, TRAB and PAZ did not have significant inhibitory efficacy on the FDCS PDOX model in the present study. Some recent studies have demonstrated how TMZ targets different pathways in various tumor systems. TMZ interacts with PD-L1 upstream targets such as the JAK/STAT pathway (Heynckes et al., 2019). TMZ also induces senescence and downregulation of DNA repair pathways in glioma cells via activation of ataxia telangiectasia and Rad3-related protein (ATR)-checkpoint kinase 1 (CHK1), cyclin-dependent kinase inhibitor 1A (p21), and nuclear factor kappa-light-chain-enhancer of activated B cells (NF-κB) pathways (Aasland et al., 2019). TMZ treatment was associated with high expression of pro-apoptotic cleaved caspase-3, PARP, phosphoinositide-3-kinase (PI3K)/protein kinase B (Akt) and extracellular signal-regulated kinase 1/2 (ERK1/2) mitogen-activated protein kinase (MAPK) pathways in musculoskeletal sarcomas (Kusabe et al., 2015). Wang et al. (2016) demonstrated that TMZ suppressed glioma cell growth by downregulating the expression of vascular endothelial growth factor C (VEGF-C) by inhibiting the ERK signaling pathway. TMZ could be delivered to the tumor site using a tumor-targeting immunoliposome nanocomplex formulation delivery system (Kim et al., 2015), and lactoferrin nanoparticles, which enhanced the therapeutic efficacy of TMZ in gliomas. (Kumari et al., 2017). The mechanism by which TMZ targets FDCS will be part of our future study.

5. Conclusion

The present study demonstrates that TMZ is effective for a PDOX model of FDCS established from a patient who failed DOX treatment. The PDOX model allowed us to precisely identify TMZ and only TMZ as effective, for this highly recalcitrant disease. The FDCS PDOX model was resistant to DOX as was the patient. The PDOX model is useful as precise individualized oncology which is most valuable for patients who failed the first- or second-line chemotherapy.

Conflict of interests

AntiCancer Inc. uses PDOX models for contract research. H.O., T.K., K.M., K.K., T.H., M.Y., Z.Z., S.R., M.B., S.W. and R.M.H. are or were unsalaried associates of AntiCancer Inc. There are no other competing financial interests.

Author contributions

H.O. and R.M.H. were involved in study conception and design. H.O., Y.T., T.K., KM., K.K., T.H., M.Y., Z.Z., S.R., M.B. and S.W. were involved in data acquisition. H.O., Y.T., T.K., KM., K.K., T.H., M.Y., Z.Z., S.R., M.B., S.W., S.D.N., T.L., M.B., S.R.S., F.K. and R.M.H. analyzed and interpreted data. H.O. and R.M.H. prepared the manuscript. S.R.S. provided critical revision of the manuscript. All authors reviewed the manuscript.

Ethical approval

All animal studies were conducted with an AntiCancer Institutional Animal Care and Use Committee (IACUC)-protocol specifically approved for this study and in accordance with the principals and procedures outlined in the National Institute of Health Guide for the Care

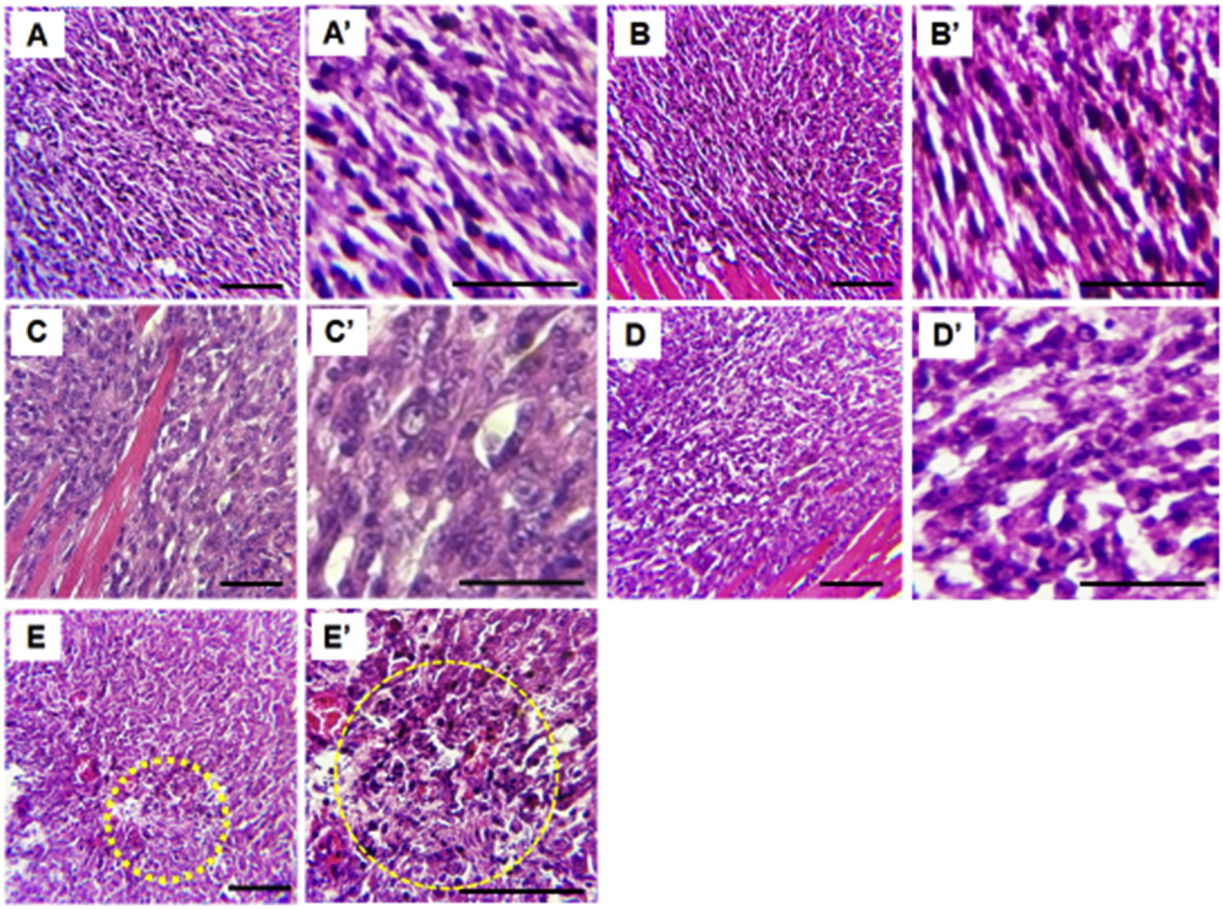

Fig. 4. Effect of treatment on tumor histlogy of the FDCS PDOX. (A, A') Untreated control (Group 1). (B, B') DOX (Group 2). (C, C') PAZ (Group 3). (D, D') TRAB (Group 4). (E, E'). TMZ (Group 5). Necrotic areas are indicated by yellow broken circles. Scale bars: 50 μm and A-F (For interpretation of the references to colour in this figure legend, the reader is referred to the web version of this article).

and Use of Animals under Assurance Number A3873-1. Written informed consent was obtained from the patient as part of a UCLA Institutional Review Board (IRB #10-001857)-approved protocol.

Acknowledgements

This manuscript is dedicated to the memory of Dr. A.R. Moossa and Dr. Sun Lee.

References

Aasland, D., Götzinger, L., Hauck, L., Berte, N., Meyer, J., Effenberger, M., Schneider, S., Reuber, E.E., Roos, W.P., Tomicic, M.T., Kaina, B., Christmann, M., 2019. Temozolomide induces senescence and repression of DNA repair pathways in glioblastoma cells via activation of ATR-CHK1, p21, and NF-κB. Cancer Res. 79 (1), 99–113.

Agaimy, A., Michal, M., Hadravsky, L., Michal, M., 2016. Follicular dendritic cell sarcoma: clinicopathologic study of 15 cases with emphasis on novel expression of MDM2, somatostatin receptor 2A, and PD-L1. Ann. Diagn. Pathol. 23, 21.

Andersen, E.F., Paxton, C.N., O'Malley, D.P., et al., 2017. Genomic analysis of follicular dendritic cell sarcoma by molecular inversion probe array reveals tumor suppressor-driven biology. Mod. Pathol. 30 (9), 1321–1334.

Anderson, M.W., Zhao, S., Freud, A.G., Czerwinski, D.K., Kohrt, H., Alizadeh, A.A., Houot, R., Azambuja, D., Biasoli, I., Morais, J.C., Spector, N., Molina-Kirsch, H.F., Warnke, R.A., Levy, R., Natkunam, Y., 2012. CD137 is expressed in follicular dendritic cell tumors and in classical Hodgkin and T-cell lymphomas: diagnostic and therapeutic implications. Am. J. Pathol. 181 (3), 795–803.

Azim, H.A., Elsedewy, E., Azim Jr, H.A., 2007. Imatinib in the treatment of follicular dendritic sarcoma: a case report and review of literature. Onkologie 30 (7), 381–384.

Biddle, D.A., Ro, J.Y., Yoon, G.S., Yong, Y.W., Ayala, A.G., Ordonez, N.G., Ro, J., 2002. Extranodal follicular dendritic cell sarcoma of the head and neck region: three new cases, with a review of the literature. Mod. Pathol. 15 (1), 50–58.

Bupathi, M., Hays, J.L., Chen, J.L., 2017. Temozolomide post pazopanib treatment failure in patients with advanced sarcoma: a case series. PLoS One 12 (11) e0188116.

Chen, T., Gopal, P., 2017. Follicular dendritic cell sarcoma. Arch. Pathol. Lab. Med. 141 (4), 596–599.

Conry, R.M., 2014a. Response of follicular dendritic cell sarcoma to gemcitabine and docetaxel: report of two cases and literature review. Clin. Sarcoma Res. 4, 6.

Conry, R.M., 2014b. Response of follicular dendritic cell sarcoma to gemcitabine and docetaxel: report of two cases and literature review. Clin. Sarcoma Res. 28 (4), 6.

Cuevas, C., Francesch, A., 2009. Development of Yondelis (trabectedin, ET-743). A semisynthetic process solves the supply problem. Nat. Prod. Rep. 26 (3), 322–337.

Dan, L.V., Huang, Y., Yang, H., Liu, S., Wang, H., Wang, M., 2014. [Diagnosis and management of nasal and pharyngeal dendritic cell tumor-case report and literature review]. Lin Er Bi Yan Hou Tou Jing Wai Ke Za Zhi 28 (8), 522–526.

Davila, J.I., Starr, J.S., Attia, S., et al., 2017. Comprehensive genomic profiling of a rare thyroid follicular dendritic cell sarcoma. Rare Tumors 9 (2), 6834.

de Lemos, M.L., Kang, I., Schaff, K., 2018. Efficacy of bevacizumab and temozolomide therapy in locally advanced, recurrent, and metastatic malignant solitary fibrous tumour: a population-based analysis. J. Oncol. Pharm. Pract., 1078155218784760.

Demetri, G.D., von Mehren, M., Jones, R.L., et al., 2016. Efficacy and safety of trabectedin or dacarbazine for metastatic liposarcoma or leiomyosarcoma after failure of conventional chemotherapy: results of a phase III randomized multicenter clinical trial. J. Clin. Oncol. 34 (8), 786–793.

Duan, G.J., Wu, F., Zhu, J., Guo, D.Y., Zhang, R., Shen, L.L., et al., 2010. Extranodal follicular dendritic cell sarcoma of the pharyngeal region: a potential diagnostic pitfall, with literature review. Am. J. Clin. Pathol. 133 (1), 49–58.

Fu, X., Hoffman, R.M., 1993. Human ovarian carcinoma metastatic models constructed in nude mice by orthotopic transplantation of histologically-intact patient specimens. Anticancer Res. 13 (2), 283–286.

Fu, X., Guadagni, F., Hoffman, R.M., 1992. A metastatic nude-mouse model of human pancreatic cancer constructed orthotopically with histologically intact patient specimens. Proc. Natl. Acad. Sci. U. S. A 89 (12), 5645–5649.

Furukawa, T., Kubota, T., Watanabe, M., Kitajima, M., Hoffman, R.M., 1993. Orthotopic transplantation of histologically intact clinical specimens of stomach cancer to nude mice: correlation of metastatic sites in mouse and individual patient donors. Int. J. Cancer 53 (4), 608–612.

Go, H., Jeon, Y.K., Huh, J., et al., 2014. Frequent detection of BRAF (V600E) mutations in histiocytic and dendritic cell neoplasms. Histopathology 65, 261–272.

Gounder, M., Desai, V., Kuk, D., Agaram, N., Arcila, M., Durham, B., Keohan, M.L., Dickson, M.A., D'Angelo, S.P., Shukla, N., Moskowitz, C., Noy, A., Maki, R.G.,

Herrera, D.A., Sanchez, A., Krishnan, A., Pourmoussa, A., Qin, L.X., Tap, W.D., 2015. Impact of surgery, radiation and systemic therapy on the outcomes of patients with dendritic cell and histiocytic sarcomas. Eur. J. Cancer 51 (16), 2413–2422.
Griffin, G.K., Sholl, L.M., Lindeman, N.I., Fletcher, C.D., Hornick, J.L., 2016. Targeted genomic sequencing of follicular dendritic cell sarcoma reveals recurrent alterations in NF-κB regulatory genes. Mod. Pathol. 29 (1), 67–74.
Grogg, K.L., Lae, M.E., Kurtin, P.J., William, M., 2004. Clusterin expression distinguishes follicular dendritic cell tumors from other dendritic cell neoplasms: report of a novel follicular dendritic cell marker and clinicopathologic data on 12 additional follicular dendritic cell tumors and 6 additional interdigitating cell tumors. Am. J. Surg. Pathol. 28 (8), 988–998.
Hassan, U., Rana, I.A., Mushtaq, S., Azam, M., Akhter, N., 2018. Follicular dendritic cell sarcoma of gastrointestinal tract: an uncommon lesion, commonly missed. J. Gastrointest. Cancer. https://doi.org/10.1007/s12029-018-0178-0.
Heynckes, S., Daka, K., Franco, P., Gaebelein, A., Frenking, J.H., Doria-Medina, R., Mader, I., Delev, D., Schnell, O., Heiland, D.H., 2019. Crosslink between Temozolomide and PD-L1 immune-checkpoint inhibition in glioblastoma multiforme. BMC Cancer 19 (1), 117.
Hiroshima, Y., Maawy, A., Zhang, Y., et al., 2014a. Metastatic recurrence in a pancreatic cancer patient derived orthotopic xenograft (PDOX) nude mouse model is inhibited by neoadjuvant chemotherapy in combination with fluorescence-guided surgery with an anti-CA 19-9-conjugated fluorophore. PLoS One 9 (12) e114310.
Hiroshima, Y., Maawy, A., Metildi, C.A., et al., 2014b. Successful fluorescence-guided surgery on human colon cancer patient-derived orthotopic xenograft mouse models using a fluorophore-conjugated anti-CEA antibody and a portable imaging system. J. Laparoendosc. Adv. Surg. Technol. A 24 (4), 241–247.
Hiroshima, Y., Maawy, A.A., Katz, M.H., et al., 2015a. Selective efficacy of zoledronic acid on metastasis in a patient-derived orthotopic xenograph (PDOX) nude-mouse model of human pancreatic cancer. J. Surg. Oncol. 111 (3), 311–315.
Hiroshima, Y., Zhang, Y., Zhang, N., et al., 2015b. Establishment of a patient-derived orthotopic Xenograft (PDOX) model of HER-2-positive cervical cancer expressing the clinical metastatic pattern. PLoS One 10 (2) e0117417.
Hiroshima, Y., Zhao, M., Zhang, Y., et al., 2015c. Tumor-targeting Salmonella typhimurium A1-R arrests a chemo-resistant patient soft-tissue sarcoma in nude mice. PLoS One 10 (8) e0134324.
Igarashi, K., Kawaguchi, K., Kiyuna, T., Murakami, T., Miwa, S., Nelson, S.D., et al., 2017a. Temozolomide combined with irinotecan caused regression in an adult pleomorphic rhabdomyosarcoma patient-derived orthotopic xenograft (PDOX) nude-mouse model. Oncotarget 8 (44), 75874–75880.
Igarashi, K., Kawaguchi, K., Murakami, T., Kiyuna, T., Miyake, K., Singh, A.S., et al., 2017b. High efficacy of Pazopanib on an undifferentiated spindle-cell sarcoma resistant to first-line therapy is identified with a patient-derived orthotopic xenograft (PDOX) nude mouse model. J. Cell. Biochem. 118 (9), 2739–2743.
Igarashi, K., Murakami, T., Kawaguchi, K., Kiyuna, T., Miyake, K., Zhang, Y., et al., 2017c. A patient-derived orthotopic xenograft (PDOX) mouse model of a cisplatinum-resistant osteosarcoma lung metastasis that was sensitive to temozolomide and trabectedin: implications for precision oncology. Oncotarget 8 (37), 62111–62119.
Igarashi, K., Kawaguchi, K., Kiyuna, T., et al., 2018a. Temozolomide regresses a doxorubicin-resistant undifferentiated spindle-cell sarcoma patient-derived orthotopic xenograft (PDOX): precision-oncology nude-mouse model matching the patient with effective therapy. J. Cell. Biochem. 119 (8), 6598–6603.
Igarashi, K., Kawaguchi, K., Kiyuna, T., Miyake, K., Miyake, M., Li, Y., et al., 2018b. Temozolomide combined with irinotecan regresses a cisplatinum-resistant relapsed osteosarcoma in a patient-derived orthotopic xenograft (PDOX) precision-oncology mouse model. Oncotarget 9 (8), 7774–7781.
Jain, P., Milgrom, S.A., Patel, K.P., Nastoupil, L., Fayad, L., Wang, M., Pinnix, C.C., Dabaja, B.S., Smith, G.L., Yu, J., Hu, S., Bueso Ramos, C.E., Kanagal-Shamanna, R., Medeiros, L.J., Oki, Y., Fowler, N., 2017. Characteristics, management, and outcomes of patients with follicular dendritic cell sarcoma. Br. J. Haematol. 178 (3), 403–412.
Karrs, J.X., Gohlke, A.L., Poklepovic, A., Oliveira, A.M., Richard, H., Pavlick, D.C., Smith, S.C., 2018. Follicular dendritic cell sarcoma with NF2 mutation. AJSP: Rev. Rep. 23 (6), 251–254.
Kawaguchi, K., Igarashi, K., Li, S., et al., 2017a. Combination treatment with recombinant methioninase enables temozolomide to arrest a BRAF V600E melanoma in a patient-derived orthotopic xenograft (PDOX) mouse model. Oncotarget 8, 85516–85525.
Kawaguchi, K., Igarashi, K., Murakami, T., et al., 2017b. Salmonella typhimurium A1-R targeting of a chemotherapy-resistant BRAF-V600E melanoma in a patient-derived orthotopic xenograft (PDOX) model is enhanced in combination with either vemurafenib or temozolomide. Cell Cycle 16 (13), 1288–1294.
Kawaguchi, K., Igarashi, K., Miyake, K., et al., 2019. Patterns of sensitivity to a panel of drugs are highly individualised for undifferentiated/unclassified soft tissue sarcoma (USTS) in patient-derived orthotopic xenograft (PDOX) nude-mouse models. J. Drug Target. 27 (2), 211–216.
Kawai, A., Yonemori, K., Takahashi, S., Araki, N., Ueda, T., 2017. Systemic therapy for Soft tissue sarcoma: proposals for the optimal use of Pazopanib, Trabectedin, and eribulin. Adv. Ther. 34 (7), 1556–1571.
Keir, S.T., Maris, J.M., Reynolds, C.P., et al., 2013. Initial testing (stage 1) of temozolomide by the pediatric preclinical testing program. Pediatr. Blood Cancer 60 (5), 783–790.
Khalid, T., Folman, R., 2005. Symptoms in cancer patients and an unusual tumor: case 3. Follicular dendritic cell sarcoma. J. Clin. Oncol. 23 (36), 9425–9426.
Kim, S.S., Rait, A., Kim, E., DeMarco, J., Pirollo, K.F., Chang, E.H., 2015. Encapsulation of temozolomide in a tumor-targeting nanocomplex enhances anti-cancer efficacy and reduces toxicity in a mouse model of glioblastoma. Cancer Lett. 369 (1), 250–258.
Kinoshita, M., Yamada, A., Sawa, D., Kamimura, S., Miyachi, M., Moritake, H., 2018. Successful treatment of metastatic alveolar rhabdomyosarcoma with MGMT gene promoter methylation by temozolomide-based combination chemotherapy. Pediatr. Blood Cancer 65 (1).
Kiyuna, T., Murakami, T., Tome, Y., et al., 2016. High efficacy of tumor-targeting Salmonella typhimurium A1-R on a doxorubicin- and dactolisib-resistant follicular dendritic-cell sarcoma in a patient-derived orthotopic xenograft PDOX nude mouse model. Oncotarget. 7 (22), 33046–33054.
Kiyuna, T., Tome, Y., Murakami, T., et al., 2018. A combination of irinotecan/cisplatinum and irinotecan/temozolomide or tumor-targeting Salmonella typhimurium A1-R arrest doxorubicin- and temozolomide-resistant myxofibrosarcoma in a PDOX mouse model. Biochem. Biophys. Res. Commun. 505 (3), 733–739.
Kumari, S., Ahsan, S.M., Kumar, J.M., et al., 2017. Overcoming blood brain barrier with a dual purpose temozolomide loaded Lactoferrin nanoparticles for combating glioma (SERP-17-12433). Sci. Rep. 7 (1), 6602.
Kusabe, Y., Kawashima, H., Ogose, A., Sasaki, T., Ariizumi, T., Hotta, T., et al., 2015. Effect of temozolomide on the viability of musculoskeletal sarcoma cells. Oncol. Lett. 10 (4), 2511–2518.
Le Cesne, A., Ray-Coquard, I., Duffaud, F., et al., 2015. Trabectedin in patients with advanced Soft tissue sarcoma: a retrospective national analysis of french sarcoma group. Eur. J. Can. 51, 742–750.
Lemech, C.R., Williams, R., Thompson, S.R., McCaughan, B., Chin, M., 2016. Treatment of breast cancer 2 (BRCA2)-mutant follicular dendritic cell sarcoma with a poly ADP-ribose polymerase (PARP) inhibitor: a case report. BMC Res. Notes 9, 386.
Lok, B.H., Gardner, E.E., Schneeberger, V.E., et al., 2017. PARP inhibitor activity correlates with SLFN11 expression and demonstrates synergy with temozolomide in small cell lung cancer. Clin. Cancer Res. 23 (2), 523–535.
Lorenzi, L., Döring, C., Rausch, T., et al., 2017. Identification of novel follicular dendritic cell sarcoma markers, FDCSP and SRGN, by whole transcriptome sequencing. Oncotarget 8 (10), 16463–16472.
Metildi, C.A., Kaushal, S., Luiken, G.A., Talamini, M.A., Hoffman, R.M., Bouvet, M., 2014. Fluorescently labeled chimeric anti-CEA antibody improves detection and resection of human colon cancer in a patient-derived orthotopic xenograft (PDOX) nude mouse model. J. Surg. Oncol. 109 (5), 451–458.
Mita, M.M., Poplin, E., Britten, C.D., Tap, W.D., Rubin, E.H., Scott, B.B., Berk, L., Rivera, V.M., Loewy, J.W., Dodion, P., Haluska, F., Sarantopoulos, J., Mita, A., Tolcher, A., 2013. Phase I/IIa trial of the mammalian target of rapamycin inhibitor ridaforolimus (AP23573; MK-8669) administered orally in patients with refractory or advanced malignancies and sarcoma. Ann. Oncol. 24 (4), 1104–1111.
Miyake, K., Murakami, T., Kiyuna, T., et al., 2017. The combination of temozolomide-irinotecan regresses a doxorubicin-resistant patient-derived orthotopic xenograft (PDOX) nude-mouse model of recurrent Ewing's sarcoma with a FUS-ERG fusion and CDKN2A deletion: direction for third-line patient therapy. Oncotarget 8 (61), 103129–103136.
Monda, L., Warnke, R., Rosai, J., 1986. A primary lymph node malignancy with features suggestive of dendritic reticulum cell differentiation. A report of 4 cases. Am. J. Pathol. 122, 562–572.
Murakami, T., Singh, A.S., Kiyuna, T., Dry, S.M., Li, Y., James, A.W., et al., 2016. Effective molecular targeting of CDK4/6 and IGF-1R in a rare FUS-ERG fusion CDKN2A-deletion doxorubicin-resistant Ewing's sarcoma patient-derived orthotopic xenograft (PDOX) nude-mouse model. Oncotarget. 7 (30), 47556–47564.
Murakami, T., Kiyuna, T., Kawaguchi, K., et al., 2017. The irony of highly-effective bacterial therapy of a patient-derived orthotopic xenograft (PDOX) model of Ewing's sarcoma, which was blocked by Ewing himself 80 years ago. Cell Cycle 16 (11), 1046–1052.
Palmerini, E., Jones, R.L., Setola, E., et al., 2018. Irinotecan and temozolomide in recurrent Ewing sarcoma: an analysis in 51 adult and pediatric patients. Acta Oncol. (Madr) 57 (7), 958–964.
Sapino, A., Cassoni, P., Ferrero, E., Bongiovanni, M., Righi, L., Fortunati, N., Crafa, P., Chiarle, R., Bussolati, G., 2003. Estrogen receptor alpha is a novel marker expressed by follicular dendritic cells in lymph nodes and tumor-associated lymphoid infiltrates. Am. J. Pathol. 163 (4), 1313–1320.
Sasaki, M., Izumi, H., Yokoyama, T., Kojima, M., Hosono, A., 2017. Follicular dendritic cell sarcoma treated with a variety of chemotherapy. Hematol. Oncol. 35 (4), 905–908.
Schoffski, P., 2012. Pazopanib in the treatment of soft tissue sarcoma. Expert Rev. Anticancer Ther. 12 (6), 711–723.
Setty, B.A., Stanek, J.R., Mascarenhas, L., et al., 2018. VIncristine, irinotecan, and temozolomide in children and adolescents with relapsed rhabdomyosarcoma. Pediatr. Blood Cancer 65, e26728.
Shinagare, A.B., Ramaiya, N.H., Jagannathan, J.P., Hornick, J.L., Swanson, R.S., 2011. Primary follicular dendritic cell sarcoma of liver treated with cyclophosphamide, doxorubicin, vincristine, and prednisone regimen and surgery. J. Clin. Oncol. 29 (35), e849–e851.
Simonetti, G., Gaviani, P., Innocenti, A., Botturi, A., Lamperti, E., Silvani, A., 2014. Update on treatment strategies for anaplastic glioma: a review of literature. Neurol. Sci. 35, 977–981.
Soriano, A.O., Thompson, M.A., Admirand, J.H., et al., 2007. Follicular dendritic cell sarcoma: a report of 14 cases and a review of the literature. Am. J. Hematol. 82 (8), 725–728.
Sun, X., Chang, K.C., Abruzzo, L.V., Lai, R., Younes, A., Jones, D., 2003. Epidermal growth factor receptor expression in follicular dendritic cells: a shared feature of follicular dendritic cell sarcoma and Castleman's disease. Hum. Pathol. 34 (9), 835.
van der Graaf, W.T., Blay, J.Y., Chawla, S.P., et al., 2012. Pazopanib for metastatic soft-tissue sarcoma (PALETTE): a randomised, double-blind, placebo-controlled phase 3 trial. Lancet 379 (9829), 1879–1886.
Walters, M., Pittelkow, M.R., Hasserjian, R.P., et al., 2018. Follicular dendritic cell sarcoma with indolent T-Lymphoblastic proliferation is associated with paraneoplastic

autoimmune multiorgan syndrome. Am. J. Surg. Pathol. 42 (12), 1647–1652.
Wang, X., Fu, X., Hoffman, R.M., 1992. A new patient-like metastatic model of human lung cancer constructed orthotopically with intact tissue via thoracotomy in immunodeficient mice. Int. J. Cancer 51 (6), 992–995.
Wang, Y., Gao, S., Wang, W., Liang, J., 2016. Temozolomide inhibits cellular growth and motility via targeting ERK signaling in glioma C6 cells. Mol. Med. Rep. 14 (6), 5732–5738.
Yamamoto, M., Zhao, M., Hiroshima, Y., et al., 2016. Efficacy of tumor-targeting Salmonella a1-r on a melanoma patient-derived orthotopic xenograft (PDOX) nude-mouse model. PLoS One 11 (8) e0160882.